Electron transport in fluid argon in combined electric and magnetic fields

P. Lamp and G. Buschhorn
Max-Planck-Institut für Physik, Werner-Heisenberg-Institut, Föhringer Ring 6, D-80805 München, Germany
(Received 13 June 1994; revised manuscript received 22 August 1994)

The transport properties of excess electrons have been measured by the time-of-flight (TOF) method in high-density gaseous and liquid argon. In addition to the electric drift field a magnetic field perpendicular to it was applied. The drift mobility μ_D and the Hall angle θ_H were measured at electric-field strengths $5 < E < 200$ V/cm and magnetic-field strengths $0 < B < 5$ T. The density of the argon was varied in the range $5.5 \le N \le 125 \times 10^{20}$ cm^{-3} in the gas phase and $93 \le N \le 173 \times 10^{20}$ cm^{-3} in the liquid phase. The experimental results in the gas phase are compared with model calculations. For $N < 70 \times 10^{20}$ cm^{-3} good agreement between measured and calculated values is found, while discrepancies are observed at higher densities. The possibility to adapt similar models based on a kinetic approach to the liquid are discussed. The difference of about 30% between the mobilities measured in the gas and liquid phase at the same density are qualitatively explained by the difference in the static structure function.

I. INTRODUCTION

The investigation of electron-transport processes in dielectric gases and liquids provides the possibility to study the effect of the arrangement of atoms or molecules on the excess electron state. By going from room temperature and normal pressure to the triple point, the density can be changed by about two orders of magnitude. The most interesting representatives of the class of dielectrics are the noble gases. In helium and neon the mobility decreases with increasing density, leading to localized electron states in the gas at high enough densities and in the liquid. For the heavier noble gases argon, krypton, and xenon, even in the liquid a high electron mobility comparable to that in the crystalline state is observed. This behavior is commonly attributed to the existence of a conduction band in the liquid. The interesting question is to follow the transition from classical single scattering in a dilute gas to multiple scattering at higher densities and the eventual formation of extended states in the liquid. In this paper we are concerned with the heavy noble gas argon, for which the input parameters (e.g., thermodynamic properties like compressibility or atomic scattering cross sections) necessary for a comparison of the experimental data with model calculations are well known.

At low densities the quantity $\mu_D N$ is a universal function of the reduced field E/N. The drift mobility μ_D is defined by $\mu_D = v_D/E$, where v_D is the electron drift velocity in an electric field E, and N is the gas density. This is the result of Boltzmann-transport theory for classical single scattering events using atomic scattering cross sections.[1] At higher densities deviations from this universality have been found.[2–4] In a restricted density range ($5 < N < 70 \times 10^{20}$ cm^{-3}) this density effect has been explained within Boltzmann-transport theory by modifying the single electron-atom scattering cross section in a density-dependent way.[4] Models based on Boltzmann-transport theory have also been applied to liquid argon.[5–8] They differ in their assumptions about the scattering processes: classical scattering with a density-modified scattering length,[5] scattering on static density fluctuations[6] or phonon scattering.[7,8] Only the first model[5] also allows us to calculate the electric-field dependence $\mu_D(E)$ as well as the thermal drift mobility $\mu_D^0 = \mu_D(E \to 0)$.

Measurements of electron transport in gaseous and liquid argon over an extended density range have been performed by Jahnke, Meyer, and Rice[9] ($56 \le N \le 211 \times 10^{20}$ cm^{-3}) and Huang and Freeman[3] ($2.0 \le N \le 211 \times 10^{20}$ cm^{-3}). However, in Ref. 9 the experimental points are on isobars, while in Ref. 3 the measurements where taken in argon vapor along the coexistence line. Thus even for gaseous argon, in both experiments a different temperature corresponds to each density. For liquid argon first results[10] on the so-called Hall mobility $\mu_H = \tan\theta_H / B$ have recently been published. The Hall angle θ_H is defined as the angle between the electron drift velocity and the electric field if a magnetic field perpendicular to the electric field is applied. This quantity provides additional information about the scattering processes relevant for the electron transport in the liquid. To our knowledge no similar measurement exists in high-density gas where the density effects are observed.

In this paper we report on systematic measurements of μ_D and θ_H at a fixed temperature of 152.5 K for gaseous argon in the density range of $5.5 \le N \le 125 \times 10^{20}$ cm^{-3}, and along the coexistence line for liquid argon in the density range $93 \le N \le 173 \times 10^{20}$ cm^{-3}. In an electron-transport measurement in dielectric gases or liquids, magnetic fields in excess of 1 T have been applied by means of a superconducting solenoid.

II. EXPERIMENT

The electron drift mobility μ_D and Hall angle θ_H have been determined simultaneously using the same drift cell. A time-of-flight (TOF) method similar to that as in our

previous experiments[4,11,12] was used. In order to measure θ_H the anode was split into two parts, each connected to a separate measuring circuit.

A. Apparatus

For measurements in magnetic fields in excess of 1 T a superconducting magnet system was used. The solenoid magnet with a large clear bore of approximately 100 mm is kept at 4.2 K in a commercial liquid-helium (LHe) cryostat. The magnet provides magnetic fields of up to 5 T with a magnetic-field variation of $<0.1\%$ within a volume of about 1 cm^3 in the center of the bore. Two thin-walled stainless-steel tubes stacked onto each other, leaving only a small gap which is evacuated fit into the bore and isolate its inner volume from the 4.2 K of the LHe. A variable-temperature insert inside the inner tube carries the measuring system.

The drift configuration is housed in a cylindrical copper cell sealed by an indium gasket. A UV-grade window glued on an INVAR collar soft soldered into the flange enables the illumination of the photocathode by the light of a Xe flashlamp. Two capillary tubes supply the cell with argon gas. The cell has been used at pressures of up to 75 bar without leakage problems.

The drift cell and its surrounding radiation shield are thermally coupled to a liquid-nitrogen (LN_2) bath. To both shield and measuring cell, a heating wire and a platinum sensor (PT100) are attached. A constant current source feeds each PT100 and a high precision resistance decade. The corresponding voltage drops are compared by a suitable amplifier circuit, and the resulting signal enters a proportional-integral-differential (PID) controller which feeds the heating wire. By setting the value of the resistance decade the temperature of the cell can be adjusted. The temperature regulation of the argon cell achieves a resolution of about 20 mK and a stability of approximately 50 mK over several hours.

The argon gas of purity 6.0 (99.9999 vol. %) is further purified by an Oxisorb filter, and enters the cell via a system of stainless-steel pipes and valves. The single parts have been thoroughly cleaned with ethanol in an ultrasonic bath, rinsed with deionized water, and dried with hot nitrogen gas. After mounting, the gas system was baked out and evacuated in several cycles. The two connections to the gas system allow us to flush the cell with argon gas continuously. For measurements in liquid argon the argon supply tubes were closed very near the cell by homemade miniature valves which could be operated from outside the cryostat. This prevents condensation of impurities from warmer parts of the gas system into the liquid argon in the measuring cell. The impurity content is estimated to be in the ppb range.

The density of the gaseous argon (given by temperature and pressure) was determined by a pressure gauge with an accuracy of ± 0.05 bar. The measurements in liquid argon were performed at the coexistence line where the density is fixed by the temperature. The density is calculated from the temperature or temperature and pressure, respectively, according to the NIST12 database of the National Institute of Standards and Technology.[13] For the given accuracy of the temperature and pressure measurement, the density is determined within an error of $<3\%$.

B. Method

The excess electrons were generated using the pulsed photoemission method as in our previous measurements,[4,11,12] by irradiating a gold photocathode with 1-μs UV pulses from a Xe flashlamp (Hamamatsu model No. L2435). The area illuminated by the UV light has a diameter of $2r_b=6$ mm. The two electrodes are of circular shape with a radius of 12.5 mm, and are placed at a distance of $d=2.3$ mm. The photocathode is held on a negative potential with respect to the anode at ground potential. The magnetic field **B** is oriented perpendicular to the electric field **E**. The anode is separated into two halves, with the dividing cut parallel to the direction of the magnetic field. The current induced by the drifting electrons in each part of the anode is integrated by means of a charge-sensitive amplifier (time constant ≈ 1 ms). The output of each amplifier is fed into a two-channel digital storage oscilloscope which is connected via GPIB bus to a personal computer. With no magnetic field applied, the measured charge for both parts of the anode equals one half of the total collected charge. A magnetic field leads to a deflection of the drifting electrons perpendicular to the magnetic field, and therefore to a difference between the signals from the two parts of the anode. A schematic drawing of the electrode configuration is shown in Fig. 1.

According to the TOF method used,[4,11,12] the analysis of the time dependence of the sum of both signals yields the drift time t_D. From the drift time the velocity component $v_{D,x}=d/t_D$ (compare Fig. 1) is calculated. For $B=0$ this leads to the drift mobility $\mu_D=v_{D,x}/E$. If a

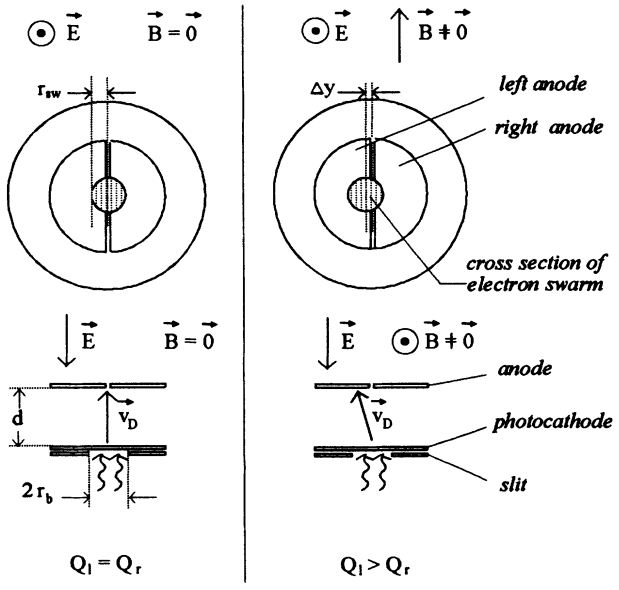

FIG. 1. Schematic drawing of the anode configuration for two different views (parallel **E** and **B**).

magnetic field is applied, the measured charges Q_l and Q_r on the two halves of the anode deduced from the amplitude of the signals allow us to determine Δy, i.e., the deflection of the electrons perpendicular to the direction of the electric field. $\tan\theta_H$ is given by the relation $\tan\theta_H = \Delta y/d$. To take care of a possible misalignment of the electrodes, the deflection Δy is calculated from the combination of the measurements at $\pm B$. The measuring error is of the order of 10%, being slightly higher for $\tan\theta_H$ compared to μ_D.

The value of Δy which can be detected is limited by the radius of the electron swarm r_b. The resolution in θ_H is a function of r_b and the drift distance d. Small r_b values and large distances d lead to a good resolution at small angles. This has been treated in detail elsewhere.[14] We just want to note that the choice of r_b and d in the present experiment allows measurements over the whole ranges of density and electric- and magnetic-field strengths reported using one single drift configuration. However, we want to stress that this is a compromise, and that our method can be adjusted to study certain regions of interest with higher precision than given here.

III. EXPERIMENTAL RESULTS

To study the transition from high-density gas to the liquid we have performed measurements in gaseous and liquid argon at several densities, at electric- and magnetic-field strengths of $5 < E < 200$ V/cm and $B < 5$ T. The density of the gas at the fixed measuring temperature at 152.5 K was adjusted by varying the pressure. The density of the liquid argon in the coexistence regime was regulated by the temperature. The thermodynamic properties of argon at the measuring points are given in Tables I (gas) and II (liquid). The full experimental data are also available in tabulated form.[15]

TABLE I. Thermodynamic properties [N: density, $S(0)$: structure factor, c: velocity of sound] and zero-field drift mobility μ_D^0 of gaseous argon at $T = 152.50$ K and the pressures p where the experimental data were taken.

p (bar)	N (10^{20} cm^{-3})[a]	$S(0)$[a]	c (m/s)[a]	μ_D^0 (cm^2/V s)[b]
67.46	125.09	1.73	329	2250
58.45	114.74	3.86	278	1710
53.20	95.48	21.51	217	800
52.61	87.40	38.08	203	570
51.89	72.94	39.14	191	240
51.19	63.20	22.75	188	200
50.52	57.31	16.67	188	190
48.79	48.25	8.27	190	220
45.73	39.31	4.80	194	240
40.64	30.30	3.00	200	300
31.65	20.17	1.94	208	433
25.36	14.94	1.60	213	555
18.28	10.01	1.35	218	780
10.75	5.52	1.17	223	1300

[a]Calculated according to NIST12 database.
[b]Experimental result of this measurement.

TABLE II. Thermodynamic properties [N: number density, p: pressure, $S(0)$: structure factor, c: velocity of sound] and zero-field drift mobility μ_D^0 of liquid argon at the temperatures T where the experimental data were taken.

T (K)	N[a] (10^{20} cm^{-3})	p[a] (bar)	$S(0)$[a]	c[a] (m/s)	μ_D^0[b] (cm^2/V s)
121.40	172.93	13.12	0.23	585	345
125.50	167.36	16.26	0.29	542	360
130.50	159.82	20.76	0.40	493	400
135.50	151.22	26.10	0.61	440	500
138.00	146.28	29.11	0.78	411	650
140.50	140.77	32.38	1.05	381	850
142.50	135.81	35.18	1.41	354	1150
143.80	132.20	37.10	1.77	336	1470
144.80	129.15	38.63	2.17	322	1680
145.70	126.15	40.05	2.69	308	1710
146.90	121.64	42.00	3.77	288	1580
148.00	116.74	43.86	5.73	269	1470
149.10	110.58	45.80	10.54	247	1080
150.10	102.64	47.62	28.29	225	695
150.70	93.36	48.75	181.20	206	400

[a]Calculated according to NIST12 database.
[b]Experimental result of this measurement.

A. Electric field

Figure 2 shows the density normalized zero-field drift mobility $\mu_D^0 N$ as a function of density for the whole density range measured. For the gas phase the well-known positive density effect[2-4] is also found in this experiment. $\mu_D N$ is no longer a universal function of E/N (Fig. 3), but $\mu_D^0 N$ increases with density.

Due to the Ramsauer-Townsend minimum in the scattering cross section, a maximum in $\mu_D N(E/N)$ for $N < 80 \times 10^{20}$ cm^{-3} occurs (Fig. 3). With increasing density $(E/N)_{max}$ decreases; here $(E/N)_{max}$ is defined as the

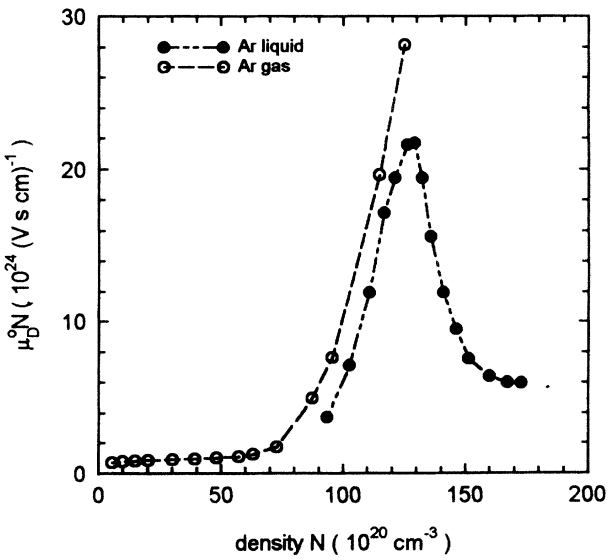

FIG. 2. Density-normalized zero-field drift mobility $\mu_D^0 N$ as a function of density for the whole density range measured.

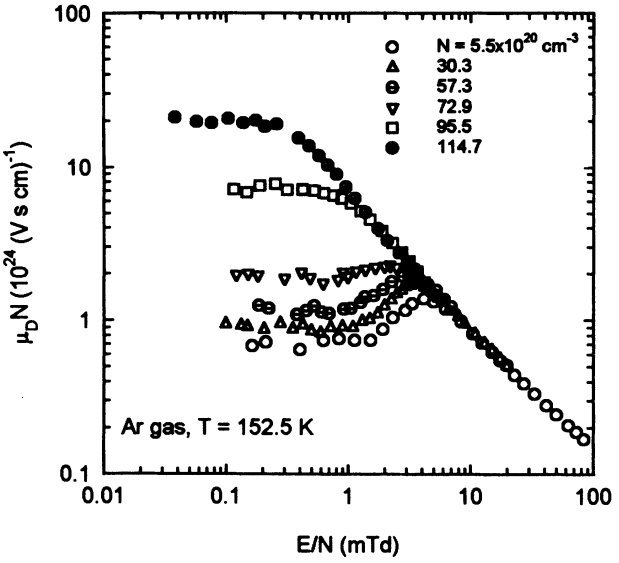

FIG. 3. Density-normalized $\mu_D N$ as a function of the reduced field for several densities in gaseous argon.

E/N value where $\mu_D N$ has its maximum value $\mu_D N_{\max}$. Furthermore, the height of the maximum (defined as the ratio of $\mu_D N_{\max}$ to $\mu_D^0 N$) decreases with density (Fig. 3). The maximum gradually disappears for densities $N > 80\times10^{20}$ cm^{-3}. For high electric-field strengths $\mu_D N(E/N)$ converges to a universal function for all densities (Fig. 3).

The most prominent effect showing up in liquid argon is the maximum in $\mu_D(N)$ (Fig. 4), already observed in a number of experiments.[3,9,11] With increasing electric-field strength this maximum decreases and shifts to lower densities. We denote as $N_{D,\max}$ the density where the drift mobility has its maximum value $\mu_{D,\max}$.

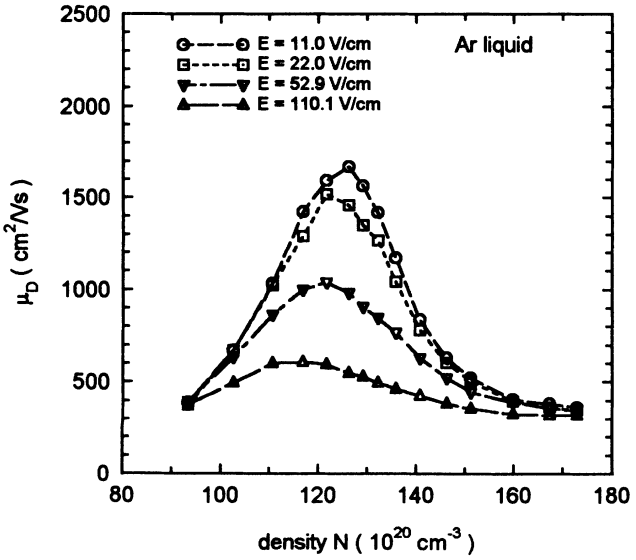

FIG. 4. Drift mobility μ_D in liquid argon as a function of density for several electric-field strengths.

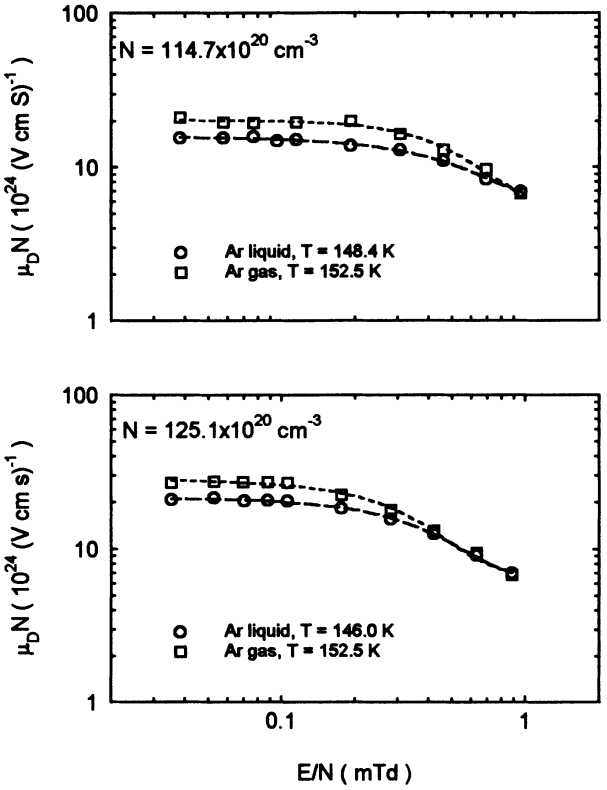

FIG. 5. Comparison of the density-normalized drift mobility $\mu_D N$ as a function of the reduced field E/N in gaseous and liquid argon at the same density.

The density region $80 < N < 125\times10^{20}$ cm^{-3} is covered by both measurements in gaseous and liquid argon. The data can be directly compared if the values $\mu_D N(E/N)$ of the liquid are interpolated to the densities measured in the gas (Fig. 5). $\mu_D N(E/N)$ shows no maximum in the liquid, similar to the observed behavior in the gas at these densities. While the qualitative behavior is the same, the gas data are about 30% higher than the liquid data.

B. Combined electric and magnetic fields

The quantity which is directly measured in an additional magnetic field is $\tan\theta_H = \Delta y/d$. With $v_{D,x} = d/t_D$ and $v_{D,y} = \Delta y/t_D$, one has

$$\tan\theta_H = v_{D,y}/v_{D,x} \ . \tag{1}$$

A Hall mobility μ_H has been introduced,[10,16] defined by the phenomenological equation

$$\mathbf{v}_D = \tilde{\mu}_D \mathbf{E} + \tilde{\mu}_D \mu_H (\mathbf{E}\times\mathbf{B}) \ . \tag{2}$$

μ_H is the characteristic quantity describing the effect of the magnetic field on the electron drift velocity; since it has the same dimension as μ_D, it is called mobility. $\tilde{\mu}_D$ is a function of the magnetic field and is connected to the drift mobility μ_D by $\mu_D = \tilde{\mu}_D(B \to 0)$. With $\mathbf{E} = (E,0,0)$ and $\mathbf{B} = (0,0,B)$, from Eqs. (2) and (1) one obtains

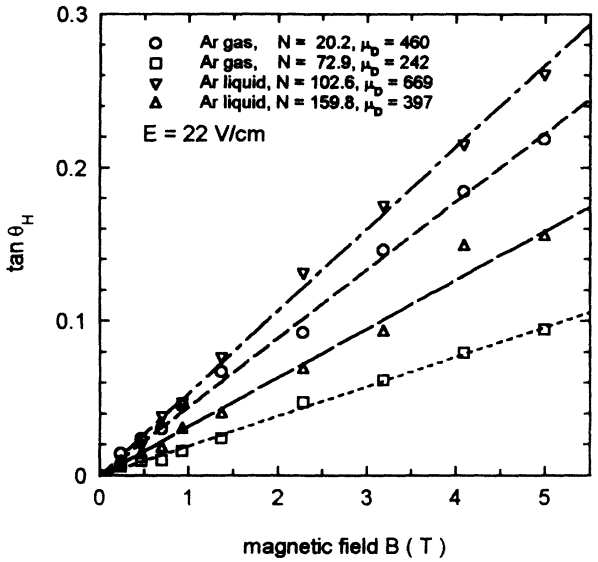

FIG. 6. $\tan\theta_H$ as a function of the magnetic field at densities where the drift mobility is low. Dashed lines are a fit of the equation $y(B)=\alpha B/(1+\beta B)$ to the data.

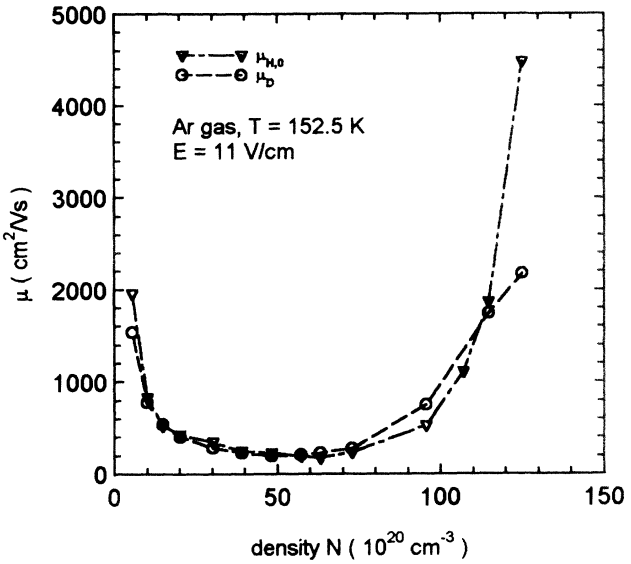

FIG. 8. Hall mobility $\mu_{H,0}$ and drift mobility μ_D as functions of density in gaseous argon.

$$\mu_H(B)=(1/B)v_{D,y}/v_{D,x}=\frac{1}{B}\tan\theta_H(B)\ . \tag{3}$$

If the Hall mobility μ_H has to be compared with the drift mobility μ_D (measured at $B=0$) the limit $\mu_{H,0}=\mu_H(B\rightarrow 0)$ has to be taken.

The experimental results show that $\tan\theta_H$ is a linear function of the magnetic field up to 5 T in argon gas, and liquid independent of density if the drift mobility is low (Fig. 6). With increasing drift mobility an increasing deviation from this linear behavior is measured (Fig. 7). We find that under all conditions studied here the experimental data of $\tan\theta_H(B)$ are very well fit by the empirical relation $y(B)=\alpha B/(1+\beta B)$ (Figs. 6 and 7). The fitted parameter α yields $\mu_{H,0}$, while β is a measure of the nonlinearity of $\tan\theta_H(B)$. Other functions, e.g., $y(B)=\alpha B/(1+\alpha B)$ or $y(B)=\alpha B/(1+\gamma B^2)$, lead to a degraded quality of the fit.

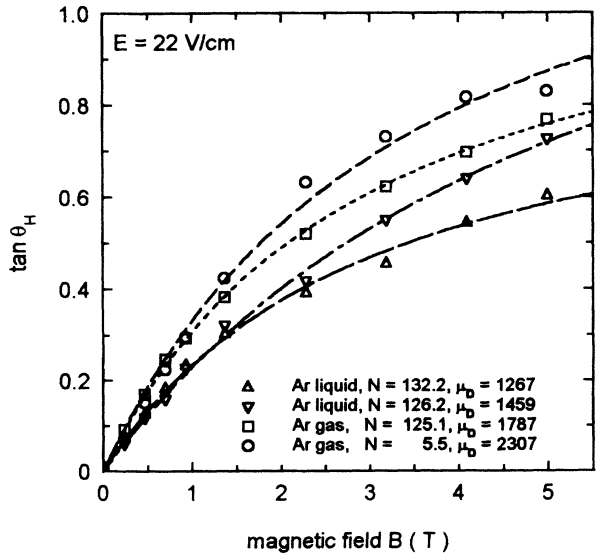

FIG. 7. $\tan\theta_H$ as a function of the magnetic field at densities where the drift mobility is high. Dashed lines are a fit of the equation $y(B)=\alpha B/(1+\beta B)$ to the data.

$\mu_{H,0}$ as function of density has the same qualitative behavior as μ_D, but results in higher absolute values. In gaseous argon for $E=11$ V/cm the ratio of $\mu_{H,0}/\mu_D$ is about 1.4 at the lowest densities measured, near 1.0 close to the critical density of 80×10^{20} cm^{-3} and up to 2.5 at the highest densities (Fig. 8). Depending on the electric-field strength in liquid argon this ratio is between 2.0 and 2.5 at densities of the μ_D maximum, and tends to unity at densities outside this maximum. In liquid argon the value $N_{H,\max}$ where $\mu_{H,0}$ has its maximum is not equal to $N_{D,\max}$ but is about 5% higher (Fig. 9). We emphasize that this shift cannot be attributed to the measuring error in the density since $\mu_{H,0}$ and μ_D have been measured at the same time and in the same cell, so that the thermodynamic conditions were identical. With increasing electric field $N_{H,\max}$ is shifted to lower densities in the same way as $N_{D,\max}$ (Fig. 10).

In the density region where gas and liquid can be compared directly, the ratio $\mu_{H,0}/\mu_D$ is approximately the same for gas and liquid, although the absolute values of $\mu_{H,0}$ and μ_D are higher in the gas.

IV. DISCUSSION

In low-density dielectric gases the electron transport is well described by the Boltzmann theory using the cross sections for single-electron-atom scattering. In dielectric gases of higher density or in liquids the formalism of Boltzmann theory is assumed still to be valid as long as

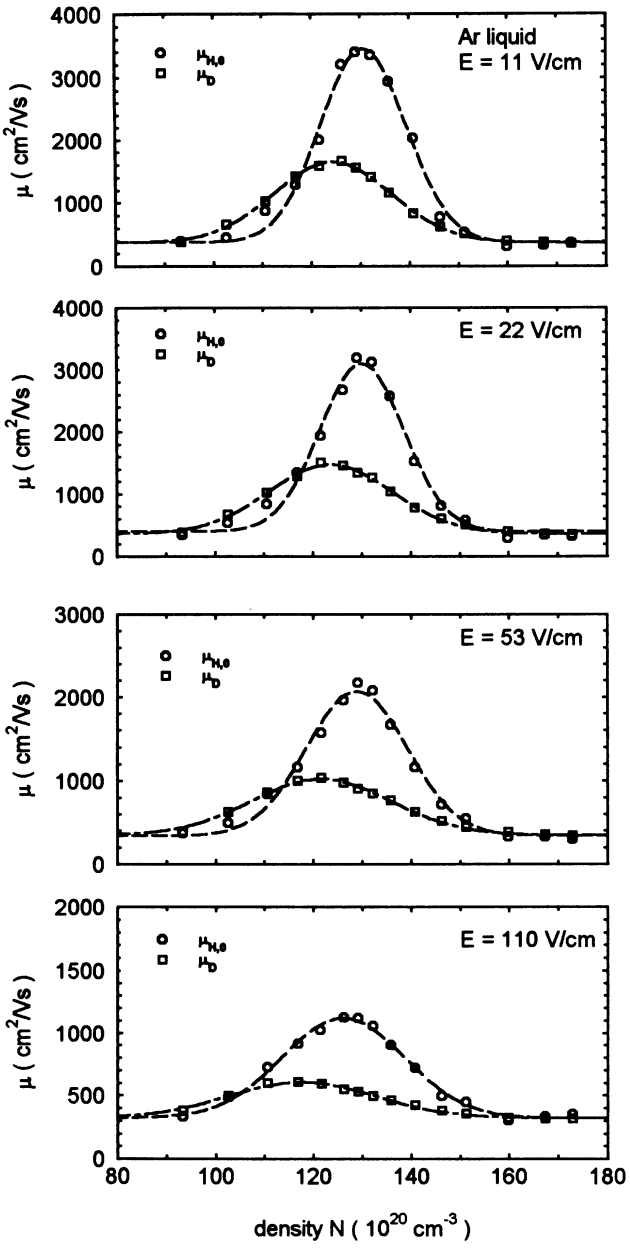

FIG. 9. Hall mobility $\mu_{H,0}$ and drift mobility μ_D as functions of density in liquid argon. Note the difference in the position of the maximum.

the mobility is high ($\mu_D > 10$ cm^2/V s), i.e., the conditions of the Boltzmann theory are fulfilled. The mean free path of the electrons has to be much larger than the electron deBroglie wavelength and the atomic diameter. In this case the apparent density effects have to be addressed to the following questions: how is the ground-state energy of the excess electron affected by the surrounding dense medium; in which way is the atomic scattering cross section modified by the increasing density; are there other scattering mechanisms (e.g., phonon scattering) that are important at higher densities or in the liquid.

For high-density argon gas a model calculation based on Boltzmann theory has been proposed by Borghesani,

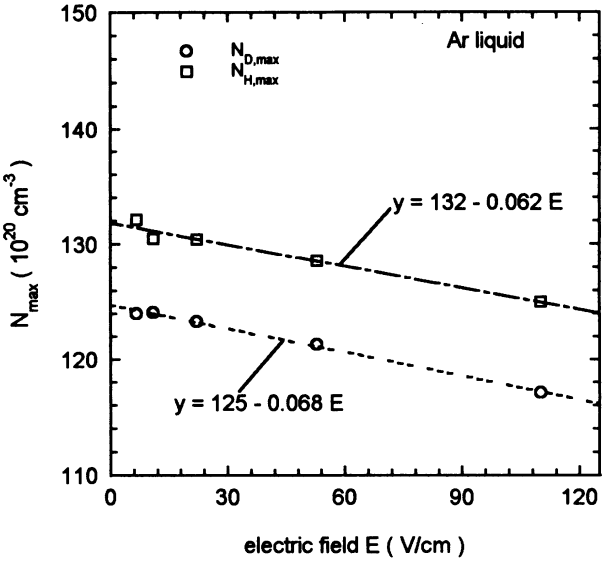

FIG. 10. Density $N_{H,\max}$ and $N_{D,\max}$ where $\mu_{H,0}(N)$ and $\mu_D(N)$ have their maximum value in liquid argon as functions of the electric-field strength.

Santini, and Lamp (BSL) (Ref. 4) which reproduces the drift mobility data up to a density of $N \approx 70\times10^{20}$ cm^{-3} very well. In the following we compare this model with the data presented here in the same density range, and make an attempt to apply it to higher densities of the gas and to the liquid.

A. Theoretical considerations

In this section we first summarize the essential features of the model of BSL,[4] and then make an extention to the case of combined electric and magnetic fields. The starting point is the drift velocity formula as given by Huxley and Crompton:[1]

$$v_D = -\frac{e}{3}\left[\frac{2}{m}\right]^{1/2}\frac{\mathbf{E}}{N}\int_0^\infty \frac{\epsilon}{\sigma_M(\epsilon)}\frac{dg(\epsilon)}{d\epsilon}d\epsilon\,, \tag{4}$$

with the Davydow-Pidduck distribution function

$$g(\epsilon) = A\exp\left\{-\int_0^\epsilon\left[\frac{e^2ME^2}{6mN^2z\sigma_M^2(z)}+k_BT\right]^{-1}dz\right\}. \tag{5}$$

Here ϵ, m, and e are the electron energy, mass, and charge, M is the molecular mass, and A is a normalization constant.

Instead of the atomic scattering cross section $\sigma_M(\epsilon)$, an effective scattering cross section $\sigma_M^*(\epsilon')$ is used where $\epsilon' = \epsilon + \epsilon_0$, and ϵ_0 is a density-dependent shift of the ground-state kinetic energy of the electron:

$$\sigma_M^*(\epsilon') = F(\epsilon')\sigma_M(\epsilon')[1+N\lambda_B F(\epsilon')\sigma_M(\epsilon')/\pi]\,. \tag{6}$$

The expression within the brackets is due to the quantum-interference effect.[17] $F(\epsilon)$ is an energy-dependent structure function which takes into account

correlations among scatterers and is given by[4]

$$F(\epsilon)=1+[S(0)-1]\times\left\{\frac{8mL^2\epsilon/\hbar^2-\ln[1+8mL^2\epsilon/\hbar^2]}{8(2mL^2\epsilon/\hbar^2)^2}\right\}. \quad (7)$$

$S(0)$ is the static structure function, and the factor $L^2=0.1l^2[S(0)-1]$ is determined by a so-called short-range correlation length of $l\simeq 10$ Å in argon.[18] In Ref. 4 the density-dependent energy shift ϵ_0 is regarded as a parameter, and is determined by fitting Eqs. (4) to (7) for $E\rightarrow 0$ to the experimental value of the extrapolated zero-field drift mobility $\mu_D^0 N$.

The density dependence of the empirical energy shift ϵ_0 was found to agree with the kinetic-energy shift T_0 of the Springett-Jortner-Cohen (SJC) model.[19] According to the SJC model the ground-state energy V_0 of the electron is given by $V_0=U_p+T_0$, where U_p is the potential energy due to the polarization of the atoms (or molecules) by the electron and T_0 is the kinetic energy which arises from the exclusion of the electron from the atomic volume (Pauli principle). In the Wigner-Seitz (WS) model the kinetic energy is given by $T_0=\hbar^2/k_0^2/2m$, with k_0 being the eigenvalue of the equation

$$\tan\{k_0[r_s-\bar{a}(k_0)]\}=k_0 r_s , \quad (8)$$

where $r_s=(3/4\pi N)^{1/3}$ is the WS radius and $\bar{a}$ is a hard-sphere radius related to the scattering cross section by $4\pi\bar{a}^2=\sigma$.[20]

The model of BSL (Ref. 4) can easily be adapted to the case of crossed electric and magnetic fields. The expressions for $v_{D,x}$ and $v_{D,y}$ were found by Huxley and Crompton:[1]

$$v_{D,x}=\frac{e}{m}EI_1, \quad v_{D,y}=\frac{e}{m}E\omega_c I_2 , \quad (9)$$

with the integrals

$$I_1=-\tfrac{2}{3}\int_0^\infty \frac{\nu(\epsilon)\epsilon^{3/2}}{\nu^2(\epsilon)+\omega_c^2}\frac{dg(\epsilon)}{d\epsilon}d\epsilon ,$$
$$I_2=-\tfrac{2}{3}\int_0^\infty \frac{\epsilon^{3/2}}{\nu^2(\epsilon)+\omega_c^2}\frac{dg(\epsilon)}{d\epsilon}d\epsilon , \quad (10)$$

where $\omega_c=eB/m$ is the cyclotron frequency, and $\nu(\epsilon)=N\sqrt{2\epsilon/m}\,\sigma_M(\epsilon)$ the mean scattering rate.

A magnetic field changes the distribution function $g(\epsilon)$ into

$$g(\epsilon)=A\exp\left\{-\int_0^\epsilon\left[\frac{e^2ME^2}{6mN^2z\sigma_M^2(z)+3m^2\omega_c^2}+k_BT\right]^{-1}dz\right\}. \quad (11)$$

In Eqs. (9)–(11) the atomic scattering cross section $\sigma_M(\epsilon)$ is to be substituted with the effective cross section $\sigma_M^*(\epsilon')$ given in Eq. (6). The measured quantity $\tan\theta_H=v_{D,y}/v_{D,x}$ is determined from the drift velocity components of Eq. (9). From Eq. (11) it can be seen that a large cyclotron frequency (high magnetic field) shifts $g(\epsilon)$ to lower energies.

B. Comparison to experiment

For comparison with the experiment, Eqs. (4)–(6) and (9)–(11) introduced in Sec. IV A have been evaluated numerically using the atomic scattering cross section given by Weyhreter *et al.*[21] Due to a lack of information about a density-dependent effective mass of the electron in gaseous or liquid argon, m has been set equal to the free-electron mass.

1. *Argon gas*

We have followed the procedure of BSL (Ref. 4) and determined for each density an ϵ_0 value from a fit to the experimental μ_D^0 data. At densities below $N\approx 70\times 10^{20}$ cm^{-3} the $\mu_D N(E/N)$ dependence calculated with this empirical ϵ_0 values is in good agreement with the experimental data (Fig. 11). ϵ_0 matches the kinetic-energy term T_0 (Fig. 12). It has to be noted that the measurements reported here have been performed at a temperature of $T=152.5$ K where $S(0)$ is much higher [Fig. 13(a)] in comparison to the temperature $T=162.7$ K of the measurements of Ref. 4. The agreement between experiment and calculation at both temperatures therefore suggests that the energy-dependent function $F(\epsilon)$ [Fig. 13(b)] takes into account the atomic arrangement of the gas at this density regime in a suitable way.

With increasing densities, however, ϵ_0 starts to deviate from T_0 (Fig. 12), and for $N>100\times 10^{20}$ cm^{-3} the measured $\mu_D^0 N$ value cannot be reproduced by variation of ϵ_0 (Fig. 14). The maximum calculated $\mu_D^0 N$ value depends on the scattering cross-section data (Fig. 14) used. Con-

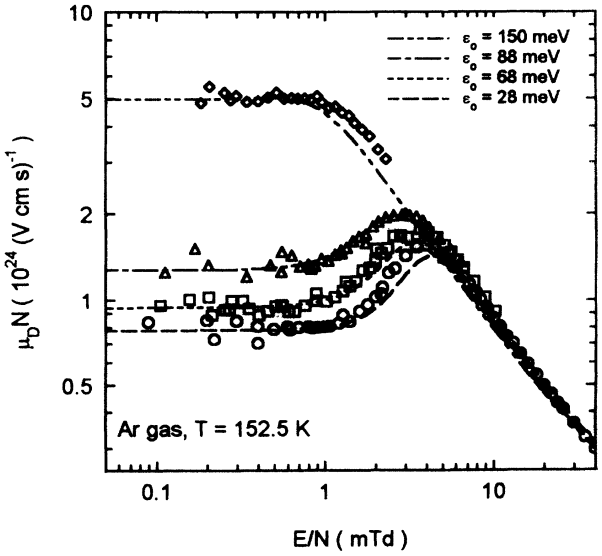

FIG. 11. $\mu_D N(E/N)$ in gaseous argon. Comparison of the experimental data and the calculation described in the text. ○, — — —; $N=10.0\times 10^{20}$ cm^{-3}; □, ----, $N=30.3$; △, — · — ·, $N=63.2$; ◇, – – –, $N=87.4$.

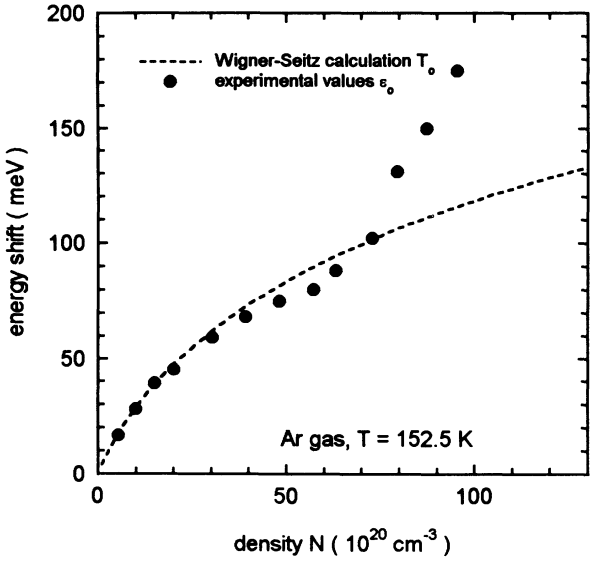

FIG. 12. Fitted values of the energy shift $\epsilon_0(N)$ compared to the kinetic-energy shift $T_0(N)$ calculated according to the Wigner-Seitz model.

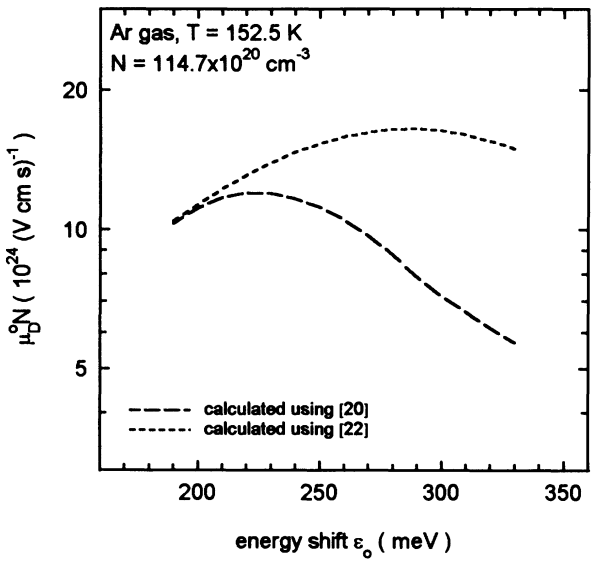

FIG. 14. Calculated values $\mu_D^0 N$ as functions of the energy shift ϵ_0 for a density of $N = 114.7 \times 10^{20}$ cm^{-3} using the different cross sections of Weyhreter *et al.*[20] and Suzuki, Taniguchi, and Tagashira.[22] The measurement yields $\mu_D^0 N \approx 20 \times 10^{24}$ (V cm s)$^{-1}$.

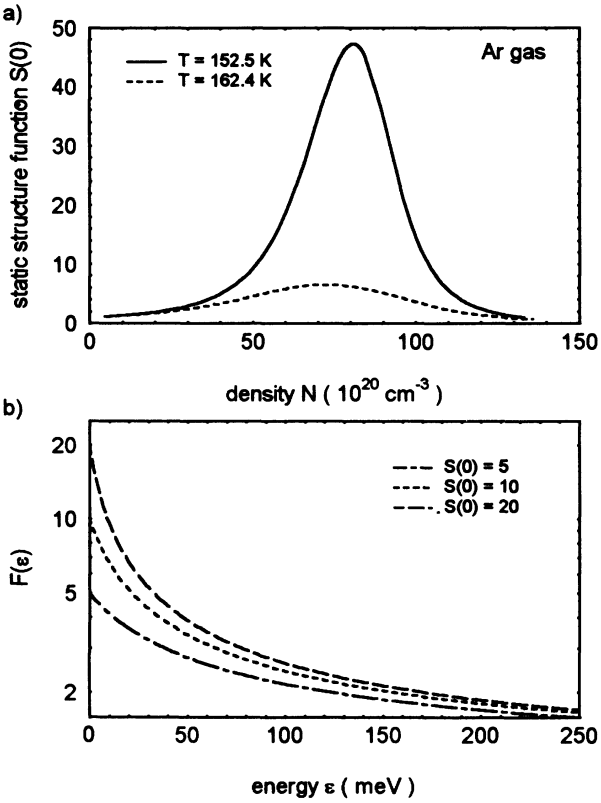

FIG. 13. (a) Static structure function $S(0)$ for $T = 162.8$ K and $T = 152.5$ K as functions of argon gas density, and (b) density-dependent correlation function $F(\epsilon)$ for different $S(0)$ values.

sidering the whole density range, the cross-section data given by Weyhreter *et al.*[21] give the best overall agreement. Nevertheless, it has to be pointed out that the atomic scattering cross sections for argon found in the literature, e.g., Refs. 21–23, differ significantly.

For densities below $N \approx 70 \times 10^{20}$ cm^{-3} the $\epsilon_0(N)$ dependence obtained can be used to calculate $\tan\theta_H(B)$. In the sense that ϵ_0 is fixed only by the drift mobility measurement, we have no adjustable parameter in the calculation of $\tan\theta_H$. The comparison between measured and calculated $\tan\theta_H(B)$ values shows good agreement (Fig. 15), giving further support to the model of BSL.[4] From Eqs. (9) and (10) it can be deduced that for fixed E/N values the quantity $\mu_H N$ should be a universal function of B/N if the scattering cross section and electron energy are independent of the density. Figure 16 shows that, similar to $\mu_D N$, $\mu_H N$ exhibits a positive density effect, i.e., $\mu_H N(B/N \to 0)$ increases with increasing density. This is in accordance with our calculation.

2. *Liquid argon*

Postponing the choice of the correct scattering cross section, Eqs. (4), (5), and (9)–(11) can in principle also be used for liquid argon. These expressions for the drift velocity or drift mobility are identical to the results of Kaneko, Usami, and Kitahara[24] derived for electron transport in liquid argon. So far, only these kinetic approaches allow us to introduce the electric-field and here also the magnetic-field dependence, although the specific form of the distribution function for not negligible electric-field strengths may be a point of discussion. The central problem is that the energy dependence of the

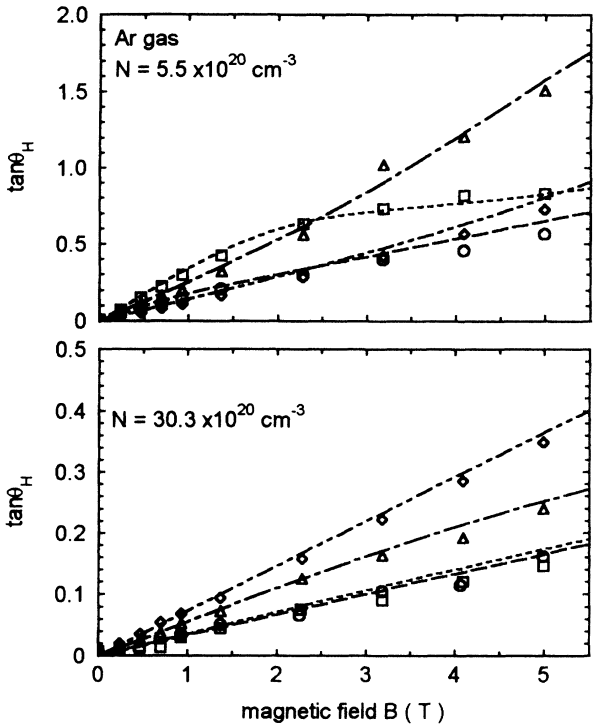

FIG. 15. $\tan\theta_H(B)$ in gaseous argon. Comparison of the experimental data (points) and the calculation (dashed lines) described in the text. ○, — — —, $E=11$ V/cm; □, ----, $E=22$ V/cm; △, —·—·—, $E=53$ V/cm; ◇, ----, $E=110$ V/cm.

scattering cross sections involved must be known in order to perform the calculations.

A simple power-law dependence of the scattering cross section ($\sigma=\sigma_0\epsilon^\gamma$) often used in solid-state physics[25] is not expected to be appropriate in this case. We found that the requirements to reproduce the qualitative behavior of $\mu_D N(E/N)$ ($\gamma>-0.5$) and $\tan\theta_H(B)$ ($\gamma<-1$) are in contradiction.[14]

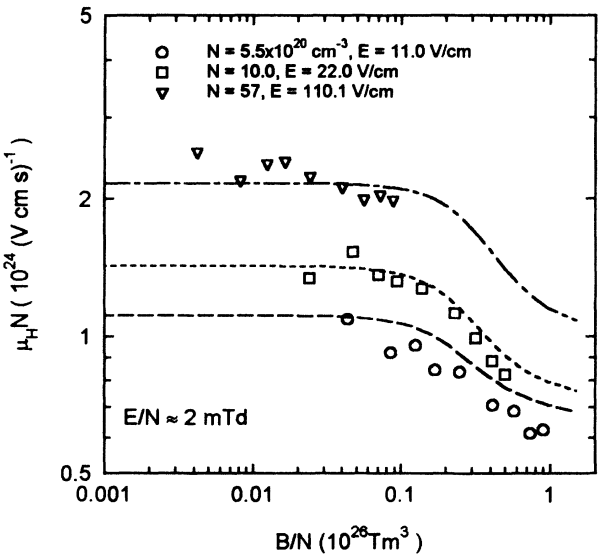

FIG. 16. $\mu_H N(B/N)$ in gaseous argon ($\mu_H=\tan\theta_H/B$) at $E/N\approx 2mTd$. The dashed lines represent the calculation described in the text.

Since an effective scattering cross section σ_M^* [Eq. (6)] successfully describes the electron transport in argon gas for $N<70\times10^{20}$ cm^{-3}, it is challenging to apply a similar ansatz to liquid argon. In order to obtain agreement with the zero-field drift mobility μ_D^0 at higher densities of the gas or in the liquid, σ_M^* was scaled by a density-dependent factor $c_0(N)$. Note that $c_0(N)$ is independent of the electric-field strength and electron energy, i.e., it has no influence on the $\mu_D N(E/N)$ dependence at fixed density. Introducing $c_0(N)$, we no longer regard the energy shift ϵ_0 as an empirical parameter, but set it equal to the kinetic-energy shift T_0 calculated according to the WS model. The astonishing result is that the dependence $\mu_D N(E/N)$ is very well described (Fig. 17). For $S(0)<1$

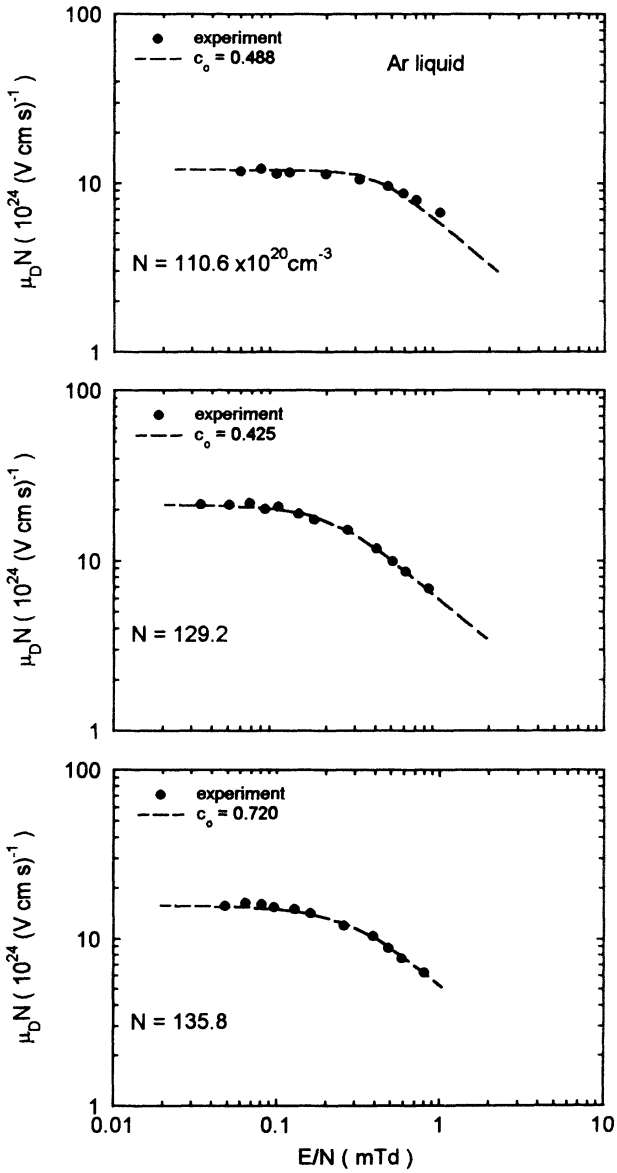

FIG. 17. $\mu_D N(E/N)$ in liquid argon at several densities. Comparison of the experimental data and a Boltzmann calculation using the effective cross section given in Eq. (6) multiplied by a constant factor c_0 adjusted to match the zero-field limit.

(in liquid argon for $N > 141 \times 10^{20}$ cm^{-3}) the function $F(\epsilon)$ in Eq. (6) is no longer defined and therefore was set to unity. The values obtained for $c_0(N)$ are in the range $0.3 < c_0(N) < 3.0$. Taking into account the limited accuracy of the atomic scattering cross section, the fact that $F(\epsilon)$ is only an approximation of an energy-dependent structure function and the neglect of a density dependence of the electron mass, i.e., an effective mass, this result is encouraging. Applying the same ansatz using the $c_0(N)$ values found above to the calculation of $\tan\theta_H(B)$, however, leads to disagreement between calculated and measured data (Fig. 18).

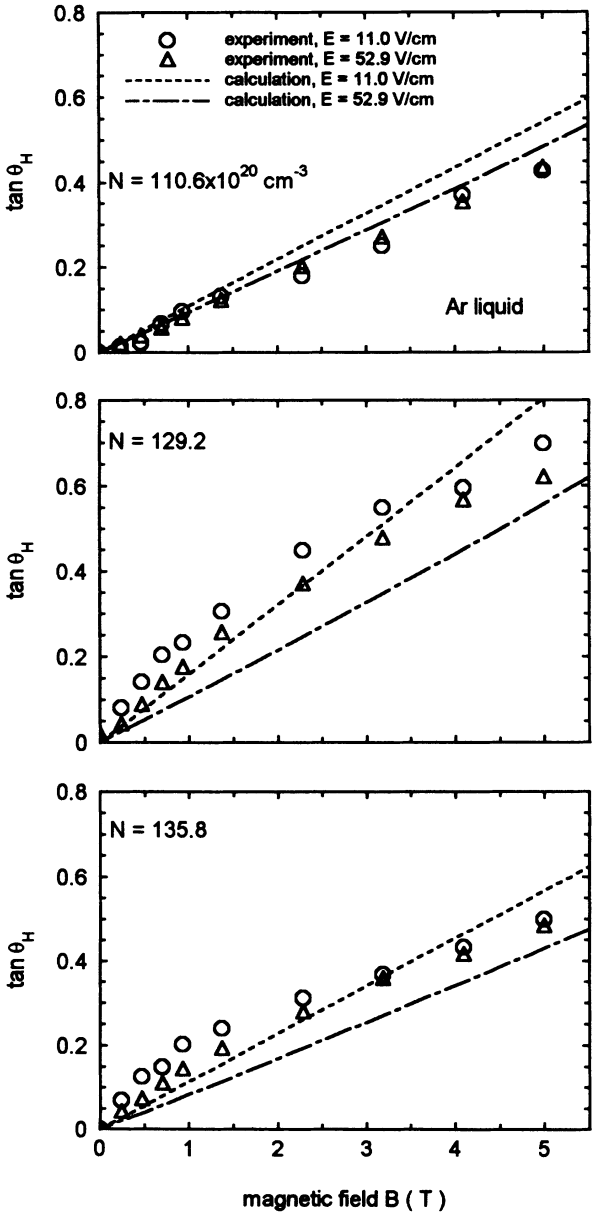

FIG. 18. $\tan\theta_H(B)$ in liquid argon at several densities. Comparison of the experimental data and a Boltzmann calculation using the effective cross section given in Eq. (6) multiplied by a constant factor c_0 adjusted to match the zero-field limit.

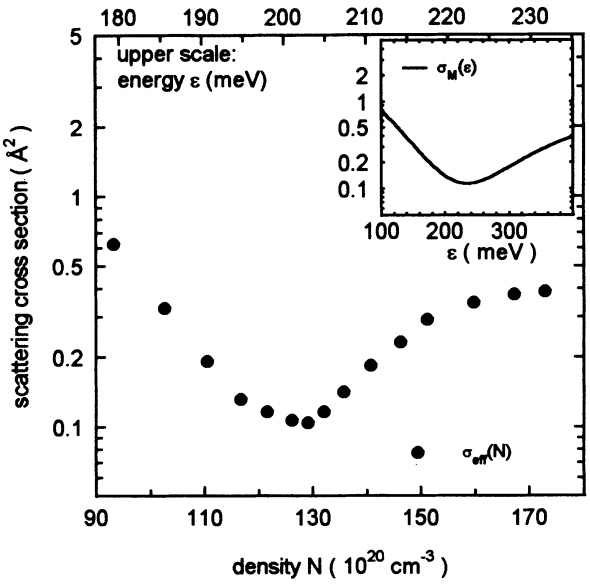

FIG. 19. Cross section $\sigma_0(N)$ necessary to reproduce the zero-field mobility $\mu_D^0(N)$ in liquid argon using the Boltzmann calculation described in the text. In the upper x scale the density has been transformed to an energy shift by calculating the kinetic-energy shift $T_0(N)$ according to the Wigner-Seitz model, and adding the thermal energy. The inset shows the atomic scattering cross section.

As a further result in liquid argon this analysis yields the density dependence of the scattering cross section of thermal electrons ($E \to 0$). This follows because $c_0(N)$ has been adjusted to match μ_D^0. In Fig. 19 we show the result $c_0(N)\sigma_M^*(N)$ calculated for $E \to 0$. The minimum in $\sigma(N)$ corresponds to the mobility maximum. If the density is transformed into energy by calculating the kinetic-energy shift $T_0(N)$ according to the WS model and adding the thermal energy $3k_BT/2$ (upper scale of Fig. 19), one finds an interesting similarity to the atomic scattering cross section shown in the inset of Fig. 19.

3. *Gaseous and liquid argon*

The measured values of the drift and Hall mobility for gaseous argon are about a factor 1.3 higher than for liquid argon at the same density (see Figs. 2 and 5). This can be understood qualitatively from the influence of the structure factor which in all models[4–8] enters the mobility formula. A higher value of $S(0)$ leads to a higher effective scattering cross section and to a lower mobility. For $N = 125.1 \times 10^{20}$ cm^{-3} one finds[13] $S(0) = 1.70$ for gaseous argon ($T = 152.5$ K) and $S(0) = 2.89$ for liquid argon ($T = 146$ K), i.e., a ratio of ~ 1.7. Calculating the drift mobility in gaseous and liquid argon by the model of BSL at $N = 125.1 \times 10^{20}$ cm^{-3} with corresponding values of $S(0)$ and T at otherwise unchanged parameters, one obtains a ratio of 1.14. This reflects the influence of the energy-dependent structure function $F(\epsilon)$ which is used instead of $S(0)$.

V. CONCLUSIONS

In this investigation we have presented systematic measurements of the drift mobility in an electric field, and of the Hall angle in a combined electric and magnetic field over a wide density range in gaseous argon at constant temperature and in liquid argon along the coexistence line. This experimental material provides a basis for comparison with model calculations of electron transport in fluid argon. In particular our measurements of the Hall angle at high magnetic fields gives further constraints for theoretical models.

In a heuristic way we have tried to explain these data within a kinetic ansatz following the model of BSL.[4] This model works well for densities $N < 70 \times 10^{20}$ cm^{-3} both for the description of $\mu_D N(E/N)$ and for $\tan\theta_H(B)$, but fails to describe the experimental data at higher densities. For liquid argon a similar approach using a power law for the energy dependence of the scattering cross section does not describe the data. An effective scattering cross section as proposed and applied by BSL,[4] which is based on the atomic scattering cross section, a density-dependent shift of the electron ground-state energy, and an energy-dependent structure function due to correlations among scatterers is able to reproduce the electric-field dependence $\mu_D N(E/N)$ if adjusted to fit $\mu_D^0 N$ by introducing an empirical factor. Using the same effective cross section, however, the calculated magnetic-field dependence of $\tan\theta_H$ does not agree with the experimental data. This demonstrates the importance of the measurement of electron transport in combined electric and magnetic fields as a constraint for models of the drift mobility.

We hope that the experimental results presented here will stimulate more refined calculations incorporating realistic models for the effective mass of the electron, and possible contributions of scattering mechanisms other than density-modified atomic scattering.

ACKNOWLEDGMENTS

We want to thank Professor A. F. Borghesani for encouraging discussions and W. Erbe for the technical support by setting up the experiment.

*Present address: ZAE Bayern, Walther-Meissner-Str. 6, D-85748 Garching, Germany.

[1]L. G. H. Huxley and R. W. Crompton, *The Diffusion and Drift of Electrons in Gases* (Wiley, New York, 1974).

[2]A. K. Bartels, Phys. Lett. **44A**, 403 (1973).

[3]S. S.-S. Huang and G. R. Freeman, Phys. Rev. A **24**, 714 (1981).

[4]A. F. Borghesani, M. Santini, and P. Lamp, Phys. Rev. A **46**, 7902 (1992).

[5]M. H. Cohen and J. Lekner, Phys. Rev. **158**, 305 (1967).

[6]S. Basak and M. H. Cohen, Phys. Rev. B **20**, 3404 (1979).

[7]G. Ascarelli, Phys. Rev. B **33**, 5825 (1986).

[8]Y. Naveh and B. Laikhtman, Phys. Rev. B **47**, 3566 (1993).

[9]J. A. Jahnke, L. Meyer, and S. A. Rice, Phys. Rev. A **3**, 734 (1971).

[10]G. Ascarelli, Phys. Rev. B **40**, 1871 (1989).

[11]R. Eibl, P. Lamp, and G. Buschhorn, Phys. Rev. B **42**, 4356 (1990).

[12]P. Lamp, R. Eibl, and G. Buschhorn, IEEE Trans. Electr. Insul. **EI-26**, 574 (1991).

[13]D. G. Friend, NIST Thermophysical Properties of Pure Fluids Database, Version 3.0, National Institute of Standards and Technology, Gaithersburg, 1992.

[14]P. Lamp, Ph.D. thesis, Technische Universität München, 1993.

[15]See AIP document no. PAPS PRBMDO-50-16824-4 for four pages of tabulated experimental data of drift mobility and Hall mobility in fluid argon. Order by PAPS number and journal reference from American Institute of Physics, Physics Auxiliary Publication Service, Carolyn Gehlbach, 500 Sunnyside Boulevard, Woodbury, New York 11797-2999. The prepaid price is $1.50 for each michrofiche (98 pages) or $5.00 for photocopies of up to 30 pages, and $0.15 for each additional page over 30 pages. Airmail additional. Make checks payable to the American Institute of Physics.

[16]R. C. Munoz and G. Ascarelli, Chem. Phys. Lett. **94**, 235 (1983).

[17]V. M. Atrazhev and I. T. Iakubov, J. Phys. D **10**, 2155 (1977).

[18]J. E. Thomas and P. W. Schmidt, J. Chem. Phys. **39**, 2506 (1963).

[19]B. E. Springett, J. Jortner, and M. H. Cohen, J. Chem. Phys. **48**, 2720 (1968).

[20]Indeed the choice of a suitable scattering length or hard core radius $\bar{a}$ is a point of discussion. The definition given here is the only one which reproduces the experimental results [A. F. Borghesani (private communication)].

[21]M. Weyhreter, B. Barzick, A. Mann, and F. Linder, Z. Phys. D **7**, 333 (1988).

[22]G. N. Haddad and T. F. O'Malley, Aust. J. Phys. **35**, 35 (1982).

[23]M. Suzuki, T. Taniguchi, and H. Tagashira, J. Phys. D **23**, 842 (1990).

[24]K. Kaneko, Y. Usami, and K. Kitahara, J. Chem. Phys. **89**, 6420 (1988).

[25]R. A. Smith, *Semiconductors* (Cambridge University Press, Cambridge, 1978).